Meson spectroscopy at VES and COMPASS

Dmitry Ryabchikov[1,2,*]
for the VES group and the COMPASS collaboration

[1]NRC Kurchatov Institute, IHEP, Protvino, Russia
[2]Technical University of Muenchen, Garching, Germany

Abstract. Diffractive production of $\pi^-\pi^-\pi^+$ and $\pi^-\pi^0\pi^0$ final states is the subject of comprehensive studies performed recently by the VES and the COMPASS experiments. COMPASS pioneered the application of novel methods of partial-wave analysis: mass-independent PWA in multiple $(m_{3\pi}, t')$-cells, mass-dependent analysis of spin-density matrices performed simultaneously in all measured t' bins, the analysis with freed shapes of $\pi^+\pi^-$ isobars. In addition, COMPASS observed a new narrow state: $a_1(1420)$. VES has world-leading data samples on $\pi^-\pi^-\pi^+$ and $\pi^-\pi^0\pi^0$, that yield compatible results and show the potential for a detailed comparison of isospin relations between different decay channels, using the PWA methods with fixed and freed shapes of $\pi\pi$ isobars.

1 Introduction

The diffractive production of 3π states is currently the subject of detailed studies by the VES [1] and the COMPASS [2] experiments. Both experiments perform an exclusive measurement of the reaction $\pi^-_{\text{beam}} N_{\text{target}} \to 3\pi N_{\text{recoil}}$, where N is a nuclear or proton target. The VES experiment runs at a beam momentum of 29 GeV/c , uses a Be target, and covers the squared four-momentum interval $0 < t' < 1.0\,(\text{GeV}/c)^2$. COMPASS uses a 190 GeV/c beam on a proton target and covers the range $0.1 < t' < 1.0\,(\text{GeV}/c)^2$.

The numbers of events, selected for the presented analysis, are 87×10^6 $\pi^-\pi^-\pi^+$ and 32×10^6 $\pi^-\pi^0\pi^0$ for VES and 46×10^6 $\pi^-\pi^-\pi^+$ and 3.5×10^6 $\pi^-\pi^0\pi^0$ for COMPASS.

The latest results of the VES analysis of the $\pi^-\pi^-\pi^+$ and $\pi^-\pi^0\pi^0$ were presented in [3–8]. VES, having compatible statistics of $\pi^-\pi^-\pi^+$ and $\pi^-\pi^0\pi^0$, presents results for both systems [3, 4]. VES reported preliminary results on a resonance-model fit of the $\pi^-\pi^0\pi^0$ data [5, 8] and a partial-wave analysis (PWA) with freed $\pi^0\pi^0$ S-wave isobar amplitudes of the $\pi^-\pi^0\pi^0$ data [8].

The COMPASS results for the $\pi^-\pi^-\pi^+$ final states were published in [9–11]. Results on $\pi^-\pi^0\pi^0$ are presented in [12, 13]. COMPASS concentrates on the analysis of $\pi^-\pi^-\pi^+$ states, and has performed a detailed PWA with 88 waves (fixed isobars), a PWA with freed $\pi^+\pi^-$ S-wave isobar amplitudes [10], and a resonance-model fit of 14 selected waves that are described simultaneously in 11 t' bins using 11 isovector resonances [9].

The short-hand notation to define 3π partial waves is

$$J^{PC}\, M^{\varepsilon}\, r\, \pi\, L, \tag{1}$$

where $J^{PC}\, M^{\varepsilon}$ are the quantum numbers of the 3π system, r is the $\pi\pi$ isobar and L is the relative orbital angular momentum between isobar r and the bachelor pion π.

*e-mail: Dmitry.Ryabchikov@ihep.ru

2 Comparison of $\pi^-\pi^-\pi^+$ and $\pi^-\pi^0\pi^0$ final states

The simultaneous analysis and comparison of $\pi^-\pi^-\pi^+$ and $\pi^-\pi^0\pi^0$ final states is important because in the isobar model, isospin symmetry relates the intensities and relative phases in the two systems.

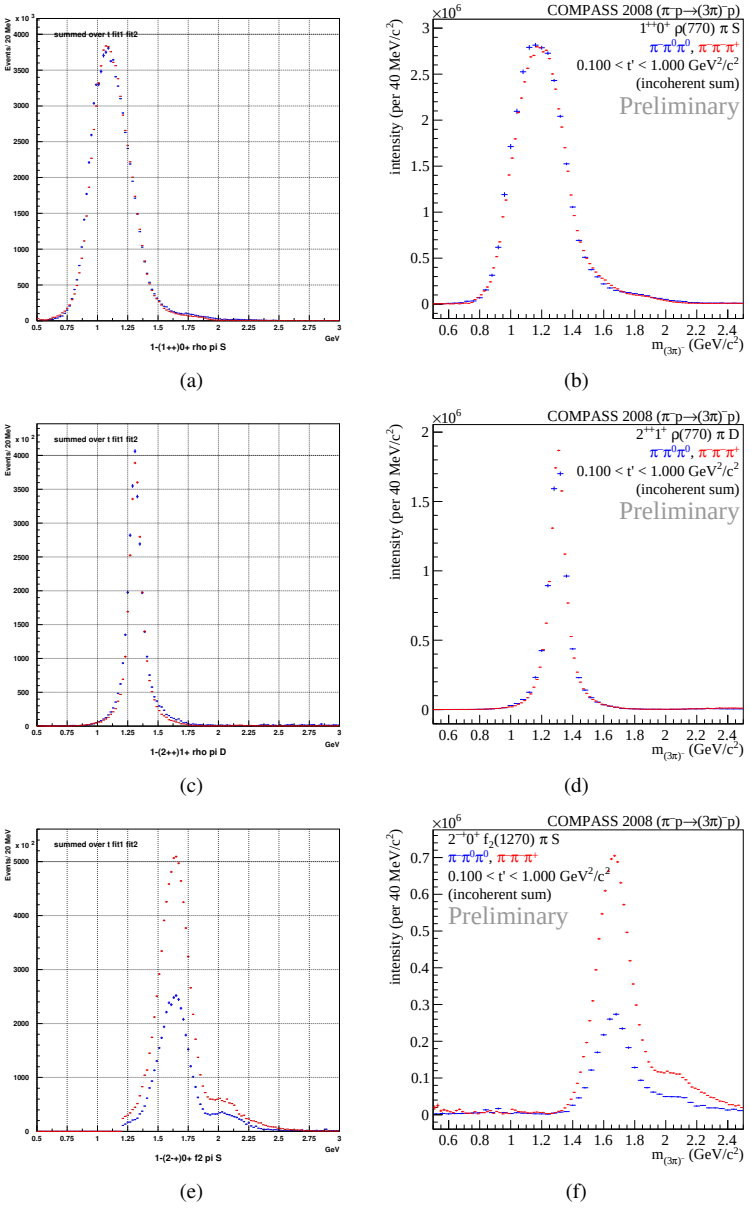

Figure 1: $1^{++}\,0^+\,\rho(770)\,\pi\,S$ intensity: VES (a), COMPASS (b). $2^{++}\,1^+\,\rho(770)\,\pi\,D$ intensity: VES (c), COMPASS (d). $2^{-+}\,0^+\,f_2(1270)\,\pi\,S$ intensity: VES (e), COMPASS (f). The $\pi^-\pi^-\pi^+$ data are shown in red, the $\pi^-\pi^0\pi^0$ data in blue.

Waves with isovector $\pi\pi$ isobars (e.g. $\rho(770)\pi$ waves) are expected to be equal between the neutral and the charged decay modes, i.e. $\mathrm{BR}(X^- \to \pi^-\pi^0\pi^0)/\mathrm{BR}(X^- \to \pi^-\pi^-\pi^+) = 1$

if we do not consider $I > 1$. Waves with isoscalar $\pi\pi$ isobars (e.g. $f_2(1270)\pi$ or $f_0(980)\pi$ waves) in the $\pi^-\pi^0\pi^0$ are expected to be half of the intensity in the $\pi^-\pi^-\pi^+$ because $\mathrm{BR}(f \to \pi^0\pi^0)/\mathrm{BR}(f \to \pi^-\pi^+) = 1/2$. However, taking into the account self-interferrence due to bose symmetrization in $\pi^-\pi^-\pi^+$, the value $\mathrm{BR}(X^- \to \pi^-\pi^0\pi^0)/\mathrm{BR}(X^- \to \pi^-\pi^-\pi^+)$ can be far away from 1/2. This happens in the case of broad $\pi\pi$ isobars such as $f_0(600)$.

Both experiments use similar approaches to analyze the data. The data are divided into set of equidistant $m_{3\pi}$ bins and non-equidistant t' bins (so-called t'-resolved analysis). The partial-wave analysis is applied independently in each ($m_{3\pi}$,t') bin, using a rank-1 spin-density matrix for dominant $\varepsilon = +1$ amplitudes. The angles of the outgoing pions are defined such that the relative phases in $\pi^-\pi^-\pi^+$ and $\pi^-\pi^0\pi^0$ are the same.

Figure 1 shows the intensities of three dominant partial waves in $m_{3\pi}$ bins, summed over t'. The $1^{++}\,0^+\,\rho(770)\,\pi\,S$ intensities from VES (figure 1(a)) and COMPASS (figure 1(b)) exhibit a broad bump that appears at lower $m_{3\pi}$ in the VES data. This points to complicated composition of the 1^{++} wave, explained by $a_1(1260)$ resonance signal and significant amount of coherent non-resonant background in the resonance-model fit of the COMPASS data [9]. The $2^{++}\,1^+\,\rho(770)\,\pi\,D$ intensity is shown in figure 1(c) for VES and in figure 1(d) for COMPASS. It shows clear peak of the $a_2(1320)$ meson. Both experiments find the expected 1:1 intensity ratio for the $\rho\pi$ decay into $\pi^-\pi^-\pi^+$ (red) and $\pi^-\pi^0\pi^0$ (blue). Figures 1(e) and 1(f) show the $2^{-+}\,0^+\,f_2(1270)\,\pi\,S$ intensity for VES and COMPASS, respectively, which is dominated by the $\pi_2(1670)$ resonance. In this case, the intensity ratio of $\pi^-\pi^0\pi^0$ to $\pi^-\pi^-\pi^+$ is close to 1/2 at 1.7 GeV/c^2, which is in agreement with the expectation from the isobar model.

The phases of the 2^{++} and 2^{-+} waves relative to the 1^{++} wave (not shown here) demonstrate a striking similarity for two experiments and for two final states. The phases also have only a weak dependence on t'. This points to the observation of the same production mechanism for the dominant resonances, even at the lower beam energies of VES, where the Reggeon exchange (for instance ρ exchange) could be significant in addition to Pomeron exchange.

3 The $a_1(1420)$

A novel resonance-like signal, the $a_1(1420)$, that appears as a narrow peak in the $1^{++}\,0^+$ $f_0(980)\,\pi\,P$ wave at about 1.4 GeV/c^2, and that is associated with a rapid phase rise was first discovered in the $\pi^-\pi^-\pi^+$ COMPASS data [11]. Resonance-model fits using 3 waves [11] and 14 waves [9] were performed, the latter yields the parameters: $m_{a_1(1420)} = 1411\,^{+4}_{-5}\,\mathrm{MeV}/c^2$ and $\Gamma_{a_1(1420)} = 161\,^{+11}_{-14}\,\mathrm{MeV}/c^2$, where uncertainties are dominated by systematics. COMPASS also observes the $a_1(1420)$ peak without modeling the line shape of the $f_0(980)$ using the freed-isobar approach [10]. VES has reported preliminary results of a resonance-model fit of the $1^{++}\,0^+\,f_0(980)\,\pi\,P$ wave using subset of the $\pi^-\pi^0\pi^0$ data [8], which are consistent with COMPASS ($m_{a_1(1420)}$ is 10 MeV/c^2 higher compared to COMPASS). The nature of the $a_1(1420)$ is highly disputed, so this phenomena needs further investigation, using different data sets.

Figures 2(a) and 2(b) show $1^{++}\,0^+\,f_0(980)\,\pi\,P$ intensity distribution for VES and COMPASS, respectively (in the latter $\pi^-\pi^-\pi^+$ is scaled to $\pi^-\pi^0\pi^0$). Figures 2(c) and 2(d) show for the lowest t' bin the relative phase between $1^{++}\,0^+\,f_0(980)\,\pi\,P$ and $1^{++}\,0^+\,\rho(770)\,\pi\,S$. Both intensities and relative phases look similar above $m_{3\pi} = 1.4$ GeV/c^2 for the two experiments. The differences at low masses could be explained by different background conditions, which can depend on beam energy, t' region and target. The current VES data, demonstrating accurate isospin relation in the peak of $a_1(1420)$ and having small statistical uncertainties in both $\pi^-\pi^-\pi^+$ and $\pi^-\pi^0\pi^0$ modes, looks very promising for further more detailed analysis, including freed-isobar methods.

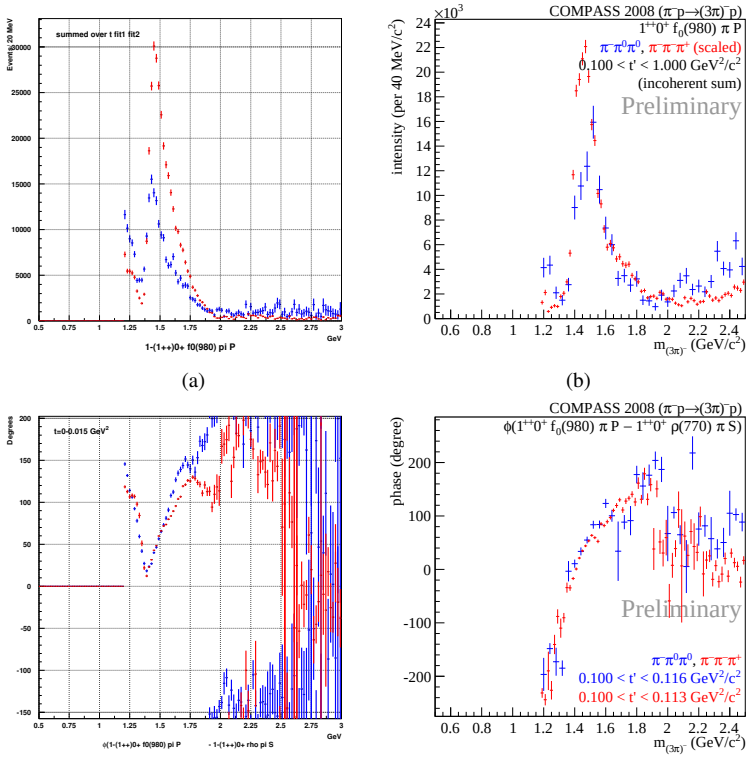

(a) (b)

(c) (d)

Figure 2: $1^{++}\,0^+\,f_0(980)\,\pi\,P$ intensity VES (a), COMPASS (b). Relative phase between the $1^{++}\,0^+\,f_0(980)\,\pi\,P$ and the $1^{++}\,0^+\,\rho(770)\,\pi\,S$ VES (c), COMPASS (d). The $\pi^-\pi^-\pi^+$ data are shown in red, the $\pi^-\pi^0\pi^0$ data in blue.

4 Freed-isobar PWA

The freed-isobar PWA is a novel approach so the method is briefly introduced. In the conventional PWA of 3π final states, the decay amplitudes (partial waves) are complex functions $\Psi_i(\tau)$ that are labeled by quantum numbers i, as is given by Eq.(1), and depending on the 3π phase-space variables τ:

$$\Psi_i(\tau) = \sum_{k=1}^{N_{\text{perm}}} \mathcal{D}_r(m_{r,k})\, F_{J_r}(m_{r,k})\, \mathcal{K}_i(\Omega_k^{\text{GJ}}, \Omega_k^{\text{HF}}). \tag{2}$$

They contain functions $\mathcal{K}_i(\Omega_k^{\text{GJ}}, \Omega_k^{\text{HF}})$ that collect all angular dependencies and depend on the angles in Gottfried-Jackson and helicity rest frames, centrifugal-barrier factors $F_{J_r}(m_r)$ and the amplitude $\mathcal{D}_r(m_r)$ describing the propagation of $\pi\pi$ isobar. Summing over index k represents the Bose symmetrization, where the kinematic variables are calculated for different combinations of the final-state pions.

In the freed-isobar method, the amplitude $\mathcal{D}(m_r)$ is presented by a set of piece-wise constant functions $\Pi_{l,r}(m_r)$ that fully cover the allowed mass range for m_r, multiplied on complex coefficients T_l:

$$\mathcal{D}(m_r) = \sum_{l}^{N_{\text{bins}}} T_l\, \Pi_{l,r}(m_r), \quad \Pi_{l,r}(m_r) = \begin{cases} 1 & \text{if } m_{r,l} \le m_r < m_{r,l+1}, \\ 0 & \text{otherwise.} \end{cases} \tag{3}$$

By substituting Eq.(3) into Eq.(2) and taking out T_l (used as fitting parameters), we construct a new set of decay amplitudes:

$$\widetilde{\Psi}_{i,l}(\tau) = \sum_{k=1}^{N_{\text{perm}}} \Pi_{l,r}(m_{r,k})\, F_{J_r}(m_{r,k})\, \mathcal{K}_i^{\varepsilon}(\Omega_k^{\text{GJ}}, \Omega_k^{\text{HF}}). \tag{4}$$

In the reflectivity basis, the amplitudes (4) are real-valued functions, without any free parameters, so the standard PWA technique can be used. Using $T_{i,l}$ as fit parameters and wave-set Eq.(4), the over-all strength of the partial wave with quantum numbers i and the isobar amplitude $\mathcal{D}(m_r)$ will be optimized.

It was found that the freed wave sets of the form of Eq. (4) contain linear-dependencies, which are exact in the limit of zero m_r bin width for $\Pi_{l,r}(m_r)$. Sets of functions were found, keeping the total 3π amplitude unchanged, when added to each $[\pi\pi]_j$ isobar amplitude. Such functions are called zero modes (ZM) [14]. These linear dependencies arise only in case of Bose-symmetrization in 3π, which breaks the orthogonality between angular amplitudes in Eq.(4). They appear when different values of L and spin j of the $\pi\pi$ isobar are used for the same $J^{PC}\, M^{\varepsilon}$. The case when the one amplitude has one ZM, is $1^{-+}\, 1^{+}\, [\pi\pi]_P\, \pi\, P$. ZM is constant function of m_r.

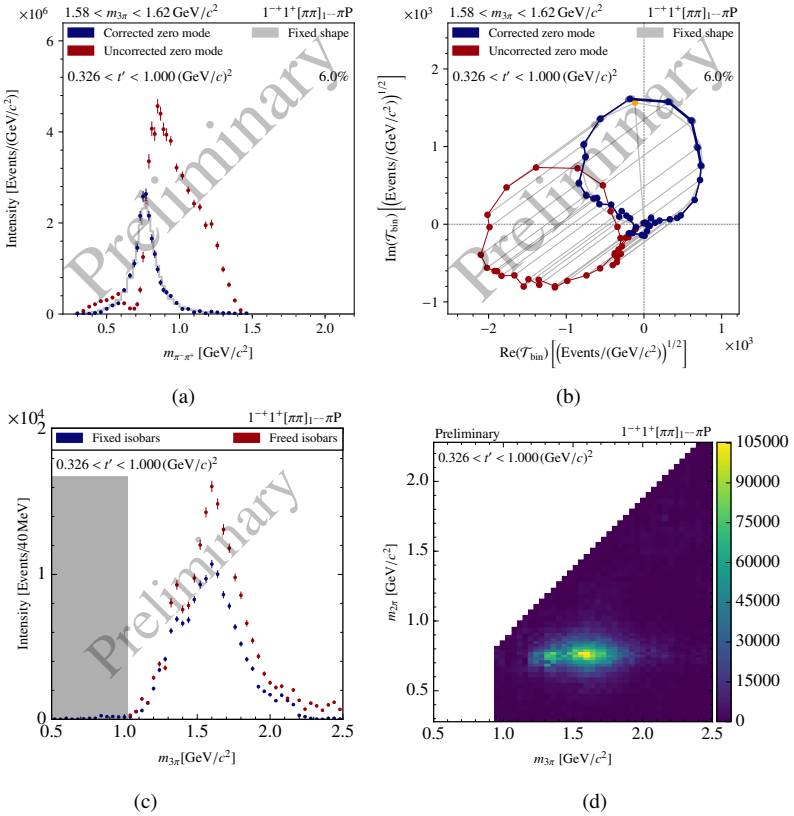

Figure 3: Intensity distribution (a) and Argand diagram (b) for the freed $[\pi\pi]_P$ amplitude before (red) and after (blue) fixing the zero mode. The $1^{-+}\, 1^{+}\, [\pi\pi]_P\, \pi\, P$ intensity in $m_{3\pi}$ bins (c) from the freed-isobar PWA (red) and the fixed-isobar PWA (blue). Intensity of 1^{-+} as a function of $m_{3\pi}$ and $m_{2\pi}$ after fixing the zero mode (d).

The latest freed-isobar PWA of the COMPASS data uses 12 waves with freed isobar amplitudes, including the spin-exotic $1^{-+}\,1^{+}\,[\pi\pi]_P\,\pi\,P$ wave [15]. Figures 3(a) and 3(b) show the intensity and Argand diagram for freed $[\pi\pi]_P$ amplitude in 1^{-+}, obtained in a single ($m_{3\pi}$,t') bin. The obtained PWA solution is shown in red, which looks very different from the expected $\rho(770)$ resonance line shape. Due to the ZM ambiguity, each data point has infinite uncertainties. Therefore, the error-bars were modified by removing the eigenvector along the ZM direction from the covariance matrix. To resolve the ambiguity, the complex amplitude of $[\pi\pi]_P$ was required to be as close as possible to Breit-Wigner amplitude of $\rho(770)$ for $m_{\pi^-\pi^+} < 1.12$ GeV/c^2, which requires fit with one complex parameter. The result of this fit is shown in figures 3(a) and 3(b) in blue and the Breit-Wigner curves are shown in gray, demonstrating nice agreement with $\rho(770)$. Figure 3(c) shows 1^{-+} intensity in all $m_{3\pi}$ bins obtained from the freed isobar fit in red, and the one from the fixed-isobar PWA in blue. Figure 3(d) shows the intensity of 1^{-+} as function of $m_{3\pi}$ and $m_{2\pi}$, after the ZM ambiguity is resolved in all $m_{3\pi}$ bins. The plot shows a clear peak at $m_{3\pi} = 1.6$ GeV/c^2 and $m_{2\pi}$=0.77 GeV/c^2 , corresponding to decay $\pi_1^-(1600) \to \rho(770)\pi^-$. This shows that $\pi_1^-(1600)$ found in the conventional analysis [9] is not an artifact due to using fixed shapes of isobars.

Conclusions and Outlook

We compare for the first time the mass-independent PWA results for the $\pi^-\pi^-\pi^+$ and $\pi^-\pi^0\pi^0$ final states that were obtained by the VES and COMPASS experiments. For both experiments, the intensities of 3 dominant partial waves exhibit the isospin relations between $\pi^-\pi^-\pi^+$ and $\pi^-\pi^0\pi^0$, that are expected for the isobar model. The $1^{++}\,0^{+}\,f_0(980)\,\pi\,P$ wave shows narrow peak in its intensity and a rapid phase rise near 1.4 GeV/c^2, attributed to the $a_1(1420)$. The VES experiment demonstrates the potential for detailed study of $a_1(1420)$ in both $\pi^-\pi^-\pi^+$ and $\pi^-\pi^0\pi^0$ final states. The extended freed-isobar fits of COMPASS $\pi^-\pi^-\pi^+$ data show the possibility of deep insight into the spin-exotic $1^{-+}\,1^{+}\,\rho(770)\,\pi\,P$ wave and the $\pi_1(1600)$.

Acknowledgments

This work was supported by RFBR grant 16-02-00737, the DFG Collaborative Research Centre/Transregio 110 and the Excellence Cluster 'Universe'.

References

[1] Yu. Khokhlov et al., EPJ Web Conf. **37**, 01029 (2012)
[2] P. Abbon et al. (COMPASS), Nucl. Instrum. Meth. **A779**, 69 (2015)
[3] I. Kachaev, D. Ryabchikov, EPJ Web Conf. **199**, 02025 (2019)
[4] I. Kachaev, D. Ryabchikov, EPJ Web Conf. **130**, 04003 (2016)
[5] D. Ryabchikov et al., AIP Conf. Proc. **1701**, 040020 (2016)
[6] I. Kachaev et al., Phys. Atom. Nucl. **78**, 1474 (2015)
[7] I. Kachaev et al., in *Proceedings, 20th International Conference on Particles and Nuclei (PANIC 14): Hamburg, Germany, August 24-29, 2014* (2014), pp. 185–189
[8] Yu. Khokhlov et al., PoS **Hadron2013**, 088 (2013)
[9] M. Aghasyan et al. (COMPASS Collaboration), Phys. Rev. D **98**, 092003 (2018)
[10] C. Adolph et al. (COMPASS Collaboration), Phys. Rev. **D95**, 032004 (2017)
[11] C. Adolph et al. (COMPASS Collaboration), Phys. Rev. Lett. **115**, 082001 (2015)
[12] S. Uhl (COMPASS), PoS **Hadron2013**, 087 (2013)
[13] S. Uhl (COMPASS), EPJ Web Conf. **164**, 07045 (2017)
[14] F. Krinner, D. Greenwald, D. Ryabchikov, B. Grube, S. Paul, Phys.Rev.D **97**, 114008 (2018)
[15] F. Krinner (COMPASS), EPJ Web Conf. **199**, 02003 (2019)